Modelling and Qualitative Analysis of the Transmission Dynamics of COVID-19 in Nigeria

*

Abstract

The novel coronavirus (COVID-19) pandemic continues despite series of control measures implemented to curtail it. Therefore, it is pertinent to study how the various proposed control measures can be effectively combined in order to stem the alarming spread of the disease and its attendant consequences. In this paper, a deterministic model for the transmission dynamics of the disease, which incorporates the impacts of the various implemented control measures, is presented. Based on the proposed model, the disease's basic reproduction number ($\mathcal{R}_0$) was derived and the equilibrium solutions were determined. It was shown that whenever $\mathcal{R}_0 \leq 1$, the model has only the disease-free equilibrium which is globally stable while in circumstances where $\mathcal{R}_0 > 1$, there exists an endemic equilibrium which is globally asymptotically stable. When the latter equilibrium state exists, the former becomes unstable. In addition, the model parameters were estimated using Nigeria's demographic and COVID-19 surveillance data. The model is simulated for different scenarios of the disease outbreak and the results suggest that the disease will die out quickly in the population if about half of the population adhere to personal protection, about half of exposed individuals are efficiently traced and about half of symptomatic individuals are promptly isolated and treated.

Keywords: COVID-19, Mathematical Modelling, Qualitative Analysis, Basis Reproduction Number, Disease Control Measures

*

1 Introduction

The coronavirus disease (COVID-19) is an infectious disease caused by the recently discovered coronavirus which belongs to a family of viruses that cause illnesses in humans and animals [16, 2]. More importantly, these viruses are common causes of respiratory infections [16]. Moreover, the latest coronavirus disease (COVID-19) outbreak was first reported in Wuhan City, Hubei Province, China on the 31st December, 2019. The disease has infected over four hundred and thirty-two million people around the world and it has resulted in about six million deaths as at 25th February, 2022 [16]. The disease pathogens primarily target the human respiratory system with symptoms including fever, cough, shortness of breath, loss of taste and sense of smell. These symptoms are similar to that of flu (influenza) or the common cold. The virus is transmitted through direct contact with respiratory droplets of an infected person usually generated through talking, coughing, and sneezing. Also, it is transmitted by touching surfaces contaminated with the virus and using the same hand to touch one's nose, mouth, or face. In addition, recent evidences portray that the disease could be contracted by inhaling air contaminated with the virus. Furthermore, it was observed that COVID-19 virus can survive on open surfaces for several hours, though simple disinfectants can be used to get rid of it.

To facilitate the understanding of mechanisms involved in the dynamics of the transmission and control of different kinds of infectious diseases in the population, several mathematical models have been proposed and analysed by researchers, see [19, 22, 23, 25, 26, 27, 31, 32, 33, 34, 35] and some of the references therein. Currently, there are series of researches on COVID-19 concerning how it spreads and effective measures to contain it [10, 1, 2, 13, 8, 3, 18, 5, 7, 4, 14, 20, 21, 24, 28, 29, 30]. For instance, Li *et al.* in [10] described the disease as a pandemic that did not have a curative vaccine yet. However, findings from the study suggest that precautionary measures like quarantine and observatory procedures could be adopted to forestall the disease spread. Although, countries around the world have put in place a range of public health and social measures to suppress or stop community transmission of the disease. Nevertheless, the World Health Organisation (WHO) published a document to provide an overview of public health and social measures that could be adopted to curtail the spread of the disease while it also proposes strategies to limit any possible harm resulting from the recommended interventions [16].

In a recent study, Adegboye *et al.* in [1] estimated the early transmissibility of COVID-19 via time-varying reproduction number based on the Bayesian method that incorporates uncertainty in the distribution of serial

interval and adjusted for disease importation. The reproduction number for each day of the outbreak was estimated using a three-weekly period while adjusting for imported cases. It was noted that COVID-19 cases in Nigeria have been remarkably lower than expected. Also, Okhuese in [13] showed that there is a chance of decline in the number of secondary infections when the ratio between the incidence rate in the population and the total number of infected population quarantined with observatory procedure decreases over time. In another study, Kucharski *et al.* in [8] assumed that the latent period of COVID-19 is equal to the incubation period and that all infected individuals will eventually become symptomatic. They found that the decline in the number of recovered humans is independent of whether the transmission occurs in first or second half of the disease incubation period.

Al-Hussein *et al.* in [3] considered a generalized SEIR model to simulate the spread of COVID-19 and forecast the future behavior of the outbreak. The seven compartmental dynamical model describes the state of the epidemic in Iraq. The best fitting for the real cumulative quarantined cases, recovered cases and death cases were obtained with the model parameters estimated using particle swarm optimization (PSO) algorithm. The country's trend of the ongoing disease and the disease epidemic inflection point were determined while the basic reproduction number, the expected cumulative number of the quarantined, exposed and infectious cases were obtained. Zhao *et al.* in [18] observed that early outbreak data obtained from Wuhan, China largely followed the exponential growth. They estimated that the mean R_0 for the disease ranges from 2.24 to 3.58, though they found that changes in reporting rate substantially affected estimates of R_0. Similarly, in a review recently conducted by Liu et al. in [11], it was found that the estimated mean of R_0 for COVID-19 is around 3.28, with a median of 2.79 and interquartile range (IQR) of 1.16. However, they stated that their estimate of R_0 is much higher than the WHO estimate of 1.95. They mentioned that the disparity in their estimated value of R_0 as compared to that of the WHO could be due to the estimation method used as well as the validity of the underlying assumptions.

In another related study, Cakir and Savas in [5] asserted that the course of the pandemic might show a very fast change in the negative direction based on the results of their mathematical model, if recommended precautions were not thoroughly adhered to or the suggested measures were not effectively implemented. Therefore, they opined that imbibing individual precautionary and social measures would play a vital role in determining the course of the pandemic. Thus, personal hygiene, social isolation, strengthening the immune system by natural and healthy nutrition, socially support, mass testing and taking care of the aged ones were recommended as measures to

check the spread of the disease.

In general, a number of preventive and control measures have been proposed to contain and, possibly, stop the spread of COVID-19. Mathematical modelling and predictions vis-à-vis their significance to epidemic prevention and control measures have been carried out by some researchers (see[7, 10]). Bulchandani *et al.* in [4] suggested that when the disease characteristics were favorable and smartphone usage high enough, smart phones could be deployed for the contact tracing phase. They found that as the usage decreases, there could be a novel contact tracing phase transition to an epidemic phase. Also, Rothana and Byrareddy in [14] proposed a simple branching-process model for COVID-19 which showed that disease immunity was possible regardless of the proportion of non-symptomatic transmission. They opined that person-to-person spread of COVID-19 infections led to the isolation of patients that were subsequently administered and a variety of treatments. As such, they suggested that special attention and efforts to protect or reduce transmission should be applied in susceptible populations including children, health care providers, and elderly people.

The foregoing notwithstanding, the coronavirus epidemic trend in Nigeria is not remarkably different from that in most other countries. As at the 25th of February 2022, there have been over two hundred and fifty-four thousand confirmed cases of the disease which have resulted in over three thousand deaths while the disease spread is still on the increase [12]. There is obviously the need for more intensive research on coronavirus in order to identify effective ways to contain its spread while the world awaits the development of potent vaccines against the virus.

This paper considers a deterministic model for the transmission dynamics of coronavirus disease with a holistic view of the impacts of implemented control measures. It is structured as follows: In section two, we present the proposed model and demonstrate that it is well posed. In section three, we carry out the qualitative analysis of the model. In section four, we numerically solve the model and simulate results for different scenarios of the disease outbreak while we also discuss findings from the simulations.

2 Proposed Mathematical Model

We propose a deterministic dynamic model for the spread of COVID-19. The model divides the population under consideration into five mutually exclusive compartments, namely Susceptible $S(t)$, Exposed $E(t)$, Infected $I(t)$, Hospitalized $H(t)$, and Recovered $R(t)$ compartments. The susceptible compartment is comprised of individuals who can be infected with the disease

if sufficiently exposed to the infection without taking adequate protective measures; the exposed compartment is made up of individuals who have been infected with the disease, though they do not exhibit the symptoms of the infection but can transmit the disease to others; the infected compartment is made up of individuals who have been infected and show symptoms of the infection; the hospitalized compartment comprises of individuals who have been confirmed to be infected by the disease based on standard test and are admitted in designated isolation centres under the care of trained medical personnel; the recovered compartment has individuals who have recovered from the infection and now possess temporary immunity against re-infection.

Thus, the proposed model for the transmission dynamics of corona-virus infection is as given in (2.1):

$$\begin{aligned}
\frac{dS}{dt} &= \Lambda + \omega R - (1-u_1)(\beta_1 E + \beta_2 H + \beta_3 I)S - \mu S, \\
\frac{dE}{dt} &= (1-u_1)(\beta_1 E + \beta_2 H + \beta_3 I)S - u_2 E - \rho E - \mu E, \\
\frac{dI}{dt} &= \rho E - u_3 I - \gamma I - (\mu + \delta_2) I, \\
\frac{dH}{dt} &= u_2 E + u_3 I - u_4 H - (\mu + \delta_1) H, \\
\frac{dR}{dt} &= \gamma I + u_4 H - \omega R - \mu R
\end{aligned} \tag{2.1}$$

It is salient to note that the total population $N(t)$ satisfies the equation

$$\frac{dN}{dt} = \Lambda - \mu N - \delta_1 H - \delta_2 I$$

The flowchart for proposed model (2.1) for the population dynamics is as given below:

Moreover, the parameters of the model are defined in Table 2.1.

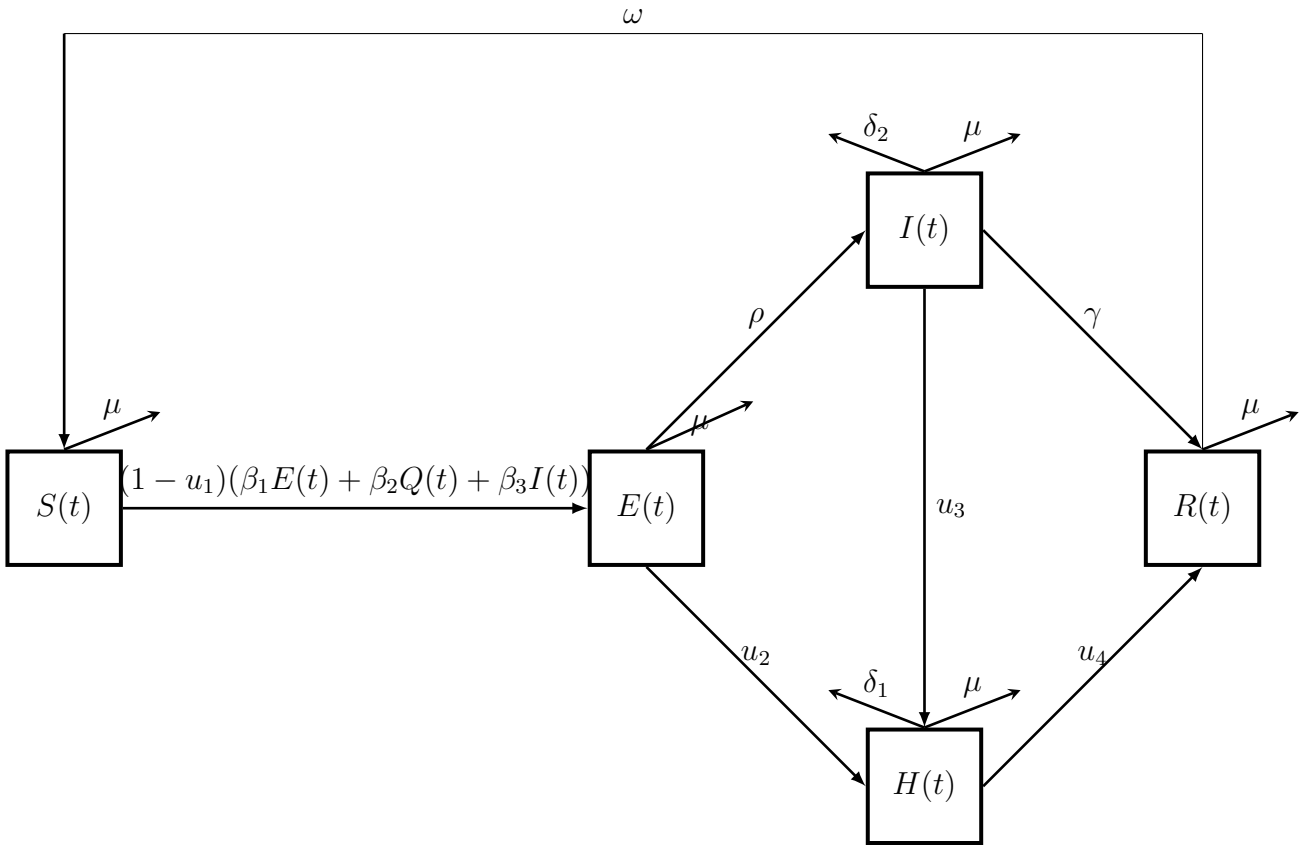

Figure 2.1: A compartmental chart for the mathematical model

Table 2.1: Description of parameters used in the model

Parameter	Description	Value	Source
Λ	recruitment rate into S class	0.0107	[15]
μ	natural death rate	0.00005	[16]
δ_1	COVID-19 induced -death rate for quarantined individuals	0.07	[12]
δ_2	COVID-19 induced -death rate for infected individuals not quarantined	0.14	[12]
β_1	transmission rate of the disease for contacts with individuals in E class.	0.0098	[12]
β_2	transmission rate of the disease for contacts with individuals in Q class.	0.0196	[12]
β_3	transmission rate of the disease for contacts with individuals in I class.	0.0294	[12]
ρ	progression rate from E class into I class.	0.155	[16]
γ	recovery rate of individuals in the I class.	0.2	[12, 16]
ω	temporary immunity waning rate for individuals in the R class	0.05	Estimate
u_1	rate of effectiveness of the implemented control measures	[0, 0.9]	Estimate
u_2	success rate of the contact tracing and testing on individuals in the E class	[0, 0.9]	Estimate
u_3	successful detection rate of symptomatic infected individuals	[0, 0.9]	Estimate
u_4	medical care success rate for hospitalized individuals	[0, 0.9]	Estimate

Note that $\lim_{t\to\infty} N(t) \leq \frac{\Lambda}{\mu}$. However, under the dynamics described by (2.1), the region Ω defined by

$$\Omega = \left\{ (S, E, I, H, R) \in \mathbb{R}^5_+ \mid S + E + I + H + R \leq \frac{\Lambda}{\mu} \right\},$$

is positively invariant.

It is important to note that $\delta_1 \leq \delta_2$; $\beta_1 \leq \beta_2 \leq \beta_3$; $u_2 \leq u_3$; $\gamma \leq u_4$ for obvious epidemiological reasons while $0 \leq u_i < 1$ for $i = 1, .., 4$, since no control measure or treatment can record 100% success rate.

Lemma 1 *The region $\mathbb{R}^5_+$ is positively-invariant for the model (2.1), i.e., the model predicts non-negative values for the state variables at any time.*

Proof 1 *Let $t_1 = sup\{t > 0 | S \geq 0,\ E \geq 0,\ I \geq 0,\ H \geq 0,\ R \geq 0,\ \in [0, t]\}$. Based on equation (2.1), we have*

$$\frac{dS}{dt} = \Lambda + \omega R - (\lambda(t) + \mu)S, \quad where \quad \lambda(t) = (1 - u_1)(\beta_1 E + \beta_2 I + \beta_3 H).$$

This is same as

$$\frac{dS}{dt} + (\lambda(t) + \mu)S = \Lambda + \omega R$$

and this implies that

$$\frac{d}{dt}\left(S(t)\exp\left(\mu t + \int_0^t \lambda(\tau)d\tau\right)\right) = (\Lambda + \omega R)\exp\left(\mu t + \int_0^t \lambda(\tau)d\tau\right).$$

Thus,

$$S(t_1)\exp\left(\mu t_1 + \int_0^{t_1} \lambda(\tau)d\tau\right) - S(0) = \int_0^{t_1} (\Lambda + \omega R(\psi))\exp\left(\mu\psi + \int_0^{\psi} \lambda(\epsilon)d\epsilon\right)d\psi$$

Hence,

$$\begin{aligned} S(t_1) &= S(0)\exp\left(-\left(\mu t_1 + \textstyle\int_0^{t_1} \lambda(\tau)d\tau\right)\right) \\ &\quad + \exp\left(-\left(\mu t_1 + \textstyle\int_0^{t_1} \lambda(\tau)d\tau\right)\right) \times \textstyle\int_0^{t_1} (\Lambda + \omega R(\psi))\exp\left(\mu\psi + \int_0^{\psi} \lambda(\epsilon)d\epsilon\right)d\psi \\ &\geq 0 \end{aligned} \tag{2.2}$$

Similarly, we can show that $E(t) \geq 0$, $I(t) \geq 0$, $H(t) \geq 0$, *and* $R(t) \geq 0$. *This completes the proof.*

The above lemma is salient to show that the model variables are continuously biologically meaningful, since population size can not be negative.

Lemma 2 *The region* Ω *is an attractor and it attracts all solutions starting in the interior of the positive orthant* $\mathbb{R}^5_+$.

Proof 2 *We use the non-negativity of the model state variables established in the preceding lemma and*

$$\frac{dN}{dt} = \Lambda - \mu N - \delta_1 H - \delta_2 I;$$

for initial conditions in $\mathbb{R}^5_+$ *and* $t \geq 0$, *to obtain* $\frac{dN}{dt} \leq \Lambda - \mu N$. *This implies that*

$$\frac{d}{dt}\big(Ne^{\mu t}\big) \leq \Lambda e^{\mu t} \Rightarrow N(t)e^{\mu t} - N(0) \leq \frac{\Lambda}{\mu}(e^{\mu t} - 1) \leq \frac{\Lambda}{\mu}e^{\mu t}.$$

So for all $t \geq 0$,

$$N(t) \leq N(0)e^{-\mu t} + \frac{\Lambda}{\mu}. \tag{2.3}$$

If $(S^*, E^*, I^*, H^*, R^*)$ *is an* Ω *limit point of an orbit in* $\mathbb{R}^5_+$*, then there is a subsequence* $t_i \to \infty$ *such that*

$$\lim_{t_i \to \infty} (S(t_i), E(t_i), I(t_i), H(t_i), R(t_i)) = (S^*, E^*, I^*, H^*, R^*).$$

Hence,

$$\lim_{t_i \to \infty} N(t_i) = N^* = S^* + E^* + I^* + H^* + R^*.$$

So, evaluating equation (2.3) *at* $t = t_i$ *and substituting into the limit as* $t_i \to \infty$*; we have that* $N^* \leq \frac{\Lambda}{\mu}$ *while* $(S^*, E^*, I^*, H^*, R^*) \in \Omega$.

Therefore, for any initial starting point $(S_0,\ E_0,\ I_0,\ H_0,\ R_0) \in \mathbb{R}^5_+$, the trajectory of solutions lies in Ω. Hence, the system is both mathematically and epidemiologically well-posed.

3 Qualitative Analysis

Qualitative analysis is used to establish the agreement between the results from the analysis and the numerical simulations. It can also be used to give graphical presentations of the behaviour of the solutions of the model.

3.1 Basic Reproduction Number

The basic reproduction number ($\mathcal{R}_0$) is the average number of secondary infections arising from an infectious individual when introduced into a population where all are susceptible to the infection. In order to derive the basic reproduction number for our model with respect to the disease, we adopt the Next Generation Matrix approach [6].

So, let X be the infected classes of the model system of differential equations (2.1), that is, $X = (E(t), I(t), H(t))$. The basic reproduction number is usually the spectral radius of the next generation matrix FV^{-1} of the model system as obtained below.

$$f_i - v_i = \begin{pmatrix} \dfrac{dE(t)}{dt} \\ \\ \dfrac{dI(t)}{dt} \\ \\ \dfrac{dH(t)}{dt} \end{pmatrix} \quad \forall\ i \in [1, 3] \tag{3.1}$$

where f_i is the rate of appearance of new infections in compartment i and v_i is the rate of transfer of individuals into compartment i. This implies that

$$f_i = \begin{pmatrix} (1-u_1)(\beta_1 E + \beta_2 H + \beta_3 I)S \\ 0 \\ 0 \end{pmatrix} \tag{3.2}$$

and

$$v_i = \begin{pmatrix} u_2 E + \rho E + \mu E \\ -\rho E + u_3 I + \gamma I + (\mu + \delta_2) I \\ -u_2 E - u_3 I + u_4 H + (\mu + \delta_1) H \end{pmatrix}. \tag{3.3}$$

The Jacobian of f at the DFE is defined as

$$F = \begin{pmatrix} \frac{\partial f_1(t)}{\partial E(t)} & \frac{\partial f_1(t)}{\partial I(t)} & \frac{\partial f_1(t)}{\partial H(t)} \\ \frac{\partial f_2(t)}{\partial E(t)} & \frac{\partial f_2(t)}{\partial I(t)} & \frac{\partial f_2(t)}{\partial H(t)} \\ \frac{\partial f_3(t)}{\partial E(t)} & \frac{\partial f_3(t)}{\partial I(t)} & \frac{\partial f_3(t)}{\partial H(t)}. \end{pmatrix} \tag{3.4}$$

So,

$$F = \begin{pmatrix} (1-u_1)\,\beta_1 S & (1-u_1)\,\beta_3 S & (1-u_1)\,\beta_2 S \\ 0 & 0 & 0 \\ 0 & 0 & 0 \end{pmatrix}. \tag{3.5}$$

Similarly, the Jacobian of v at DFE denoted by V is defined as:

$$V = \begin{pmatrix} \frac{\partial v_1(t)}{\partial E(t)} & \frac{\partial v_1(t)}{\partial I(t)} & \frac{\partial v_1(t)}{\partial H(t)} \\ \frac{\partial v_2(t)}{\partial E(t)} & \frac{\partial v_2(t)}{\partial I(t)} & \frac{\partial v_2(t)}{\partial H(t)} \\ \frac{\partial v_3(t)}{\partial E(t)} & \frac{\partial v_3(t)}{\partial I(t)} & \frac{\partial v_3(t)}{\partial H(t)} \end{pmatrix} = \begin{pmatrix} \mu + \rho + u_2 & 0 & 0 \\ -\rho & \gamma + u_3 + \mu + \delta_1 & 0 \\ -u_2 & -u_3 & u_4 + \mu + \delta_1 \end{pmatrix}. \tag{3.6}$$

This implies that

$$V^{-1} = \begin{pmatrix} (\mu+\rho+u_2)^{-1} & 0 & 0 \\ \frac{\rho}{(\mu+\rho+u_2)(\gamma+u_3+\mu+\delta_1)} & (\gamma+u_3+\mu+\delta_1)^{-1} & 0 \\ \frac{\mu\,u_2+\rho\,u_3+\gamma\,u_2+u_2u_3+u_2\delta_1}{(\mu+\rho+u_2)(\gamma+u_3+\mu+\delta_1)(u_4+\mu+\delta_1)} & \frac{u_3}{(\gamma+u_3+\mu+\delta_1)(u_4+\mu+\delta_1)} & (u_4+\mu+\delta_1)^{-1} \end{pmatrix}. \tag{3.7}$$

Hence, the basic reproduction number ($\mathcal{R}_0$) is obtained as the dominant eigenvalue in the next generation matrix $G = FV^{-1}$. Therefore, $\mathcal{R}_0$ is as stated

$$\mathcal{R}_0 = \frac{\Lambda(1-u_1)}{\mu}\left(\frac{\beta_1}{x} + \frac{\beta_2(\rho u_3 + y u_2)}{xyz} + \frac{\beta_3\rho}{xy}\right)$$

while $x, y, and\ z$ are as defined in the preceding subsection.

3.2 Steady States

The steady states of the model are obtained by setting each of the left-hand side expressions of the system of differential equations (2.1) to zero and solving the resulting system of equations simultaneously such that we have the following.

- the disease-free equilibrium solution:

$$\varepsilon_1 = \left(S^* = \frac{\Lambda}{\mu}, E^* = 0, I^* = 0, H^* = 0, R^* = 0\right);$$

- the endemic equilibrium solution:

$$\varepsilon_2 = \left(S^{**} = \frac{xyz}{\beta_1 yz + \beta_2\rho u_3 + \beta_2 u_2 y + \beta_3\rho z}, E^{**} = \frac{v}{Dx}(\mathcal{R}_0 - 1), I^{**} = \frac{\rho v}{Dxy}(\mathcal{R}_0 - 1), \tag{3.8}$$

$$H^{**} = \frac{v(\rho u_3 + u_2 y)}{Dxyz}(\mathcal{R}_0 - 1), R^{**} = \frac{\rho u_3 u_4 + \rho\gamma z + u_2 u_4 y}{Dxyz}(\mathcal{R}_0 - 1)\right) \tag{3.9}$$

where $v = \mu + \omega$; $x = \mu + \rho + u_2$; $y = \mu + \gamma + \delta_2 + u_3$; $z = \mu + \delta_1 + u_4$;

$D = (\beta_1 yz + \beta_2\rho u_3 + \beta_2 u_2 y + \beta_3\rho z)\,(vxyz - \omega(\rho u_3 u_4 + \rho\gamma z + u_2 u_4 y))$;

and

$$\mathcal{R}_0 = \frac{\Lambda(1-u_1)}{\mu}\left(\frac{\beta_1}{x} + \frac{\beta_2(\rho u_3 + y u_2)}{xyz} + \frac{\beta_3\rho}{xy}\right).$$

3.3 Stability Analysis

Theorem 1 *The model* (2.1) *has the disease free equilibrium* (ε_1) *as its only equilibrium solution whenever* $\mathcal{R}_0 < 1$ *and it is globally asymptotically stable (GAS).*

Proof 3 *Suppose* $\mathcal{R}_0 < 1$*, then the model has only the disease-free equilibrium* (ε_1) *as its only equilibrium. So, we only need to show that* (ε_1) *is GAS. Let us consider a Lyapunov function* $\mathcal{V}$ *of the form below:*

$$\mathcal{V}(S, E, I, H, R) = C_1E + C_2I + C_3H. \tag{3.10}$$

On the differentiation of $\mathcal{V}$ *with respect to* t *in* (3.10)*, we have :*

$$\begin{aligned}
\frac{d\mathcal{V}}{dt} &= C_1E' + C_2I' + C_3H' \\
&= C_1((1-u_1)(\beta_1E + \beta_2H + \beta_3I)S - u_2E - \rho E - \mu E) \\
&\quad + C_2(\rho E - u_3I - \gamma I - (\mu + \delta_2)I) \\
&\quad + C_3(u_2E + u_3I - u_4H - (\mu + \delta_1)H), \\
&\leq C_1((1-u_1)(\beta_1E + \beta_2H + \beta_3I)(\tfrac{\Lambda}{\mu}) - u_2E - \rho E - \mu E) \\
&\quad + C_2(\rho E - u_3I - \gamma I - (\mu + \delta_2)I) \\
&\quad + C_3(u_2E + u_3I - u_4H - (\mu + \delta_1)H); \quad Taking\ S = S^* = \tfrac{\Lambda}{\mu}, \\
&\leq \Big(C_1(1-u_1)(\tfrac{\Lambda}{\mu})\beta_1 + C_2\rho + C_3u_2 - C_1(\mu + \rho + u_2)\Big)E \\
&\quad + \Big(C_1(1-u_1)(\tfrac{\Lambda}{\mu})\beta_2 - C_3(\mu + u_4 + \delta_1)\Big)H \\
&\quad + \Big(C_1(1-u_1)(\tfrac{\Lambda}{\mu})\beta_3 + C_3u_3 - C_2(\mu + \gamma + u_3 + \delta_2)\Big)I, \\
&\leq (\mathcal{R}_0 - 1)E, \quad where\ C_1 = 1,\ C_2 = \tfrac{\Lambda(1-u_1)(\beta_3(u_4+\delta_1+\mu)+\beta_2u_3)}{\mu(\mu+u_4+\delta_1)(\mu+\gamma+u_3+\delta_2)}, \\
&\quad and\ C_3 = \tfrac{\Lambda(1-u_1)\beta_2}{\mu(\mu+u_4+\delta_1)}.
\end{aligned} \tag{3.11}$$

In view of the foregoing, it is imperative to note that $\mathcal{V}' = 0$ *only when* $E = 0$*. Moreover, the substitution of* $E = 0,\ I = 0,\ H = 0,$ *and* $R = 0$ *into the model system of equations indicates that* $S \to \frac{\Lambda}{\mu}$ *as* $t \to \infty$*. Hence, the maximum invariant set in* $\{(S,\ E,\ I,\ H,\ R) \in \Omega | \mathcal{V}' \leq 0\}$ *is a singleton set* $\{\varepsilon_1\}$*. Based on LaSalle's invariance principle [9],* ε_1 *is globally asymptotically stable whenever* $\mathcal{R}_0 < 1$*.*

It is worthy of note that when $\mathcal{R}_0 = 1$, the model will still have only the disease-free equilibrium, though it will loose its asymptotic stability and be neutrally stable.

Theorem 2 *If* $\mathcal{R}_0 > 1$*, then the model* (2.1) *has an endemic equilibrium* ε_2 *(in addition to the disease free equilibrium) and it is globally asymptotically stable.*

Proof 4 *Suppose $\mathcal{R}_0 > 1$, then there exists the Endemic equilibrium ε_2, which is different from the disease-free equilibrium. Then, there is the need to show that it is GAS. In order to establish global stability of ε_2 , we shall consider a Lyapunov function $\mathcal{V}(S, E, I, H, R)$ of the form below:*

$$\mathcal{V} = \frac{1}{2}\left((S - S^{**})^2 + (E - E^{**})^2 + (I - I^{**})^2 + (H - H^{**})^2 + (R - R^{**})^2\right). \tag{3.12}$$

It is worth mentioning that at the endemic equilibrium point, the following set of equations hold:

$$\begin{aligned}
\Lambda + \omega R^{**} &= (1 - u_1)(\beta_1 E^{**} + \beta_2 H^{**} + \beta_3 I^{**})S^{**} + \mu S^{**},\\
(1 - u_1)(\beta_1 E^{**} + \beta_2 H^{**} + \beta_3 I^{**})S^{**} &= (u_2 + \rho + \mu)E^{**},\\
\rho E^{**} &= (u_3 + \gamma I + \mu + \delta_2)I^{**},\\
u_2 E^{**} + u_3 I^{**} &= (u_4 + \mu + \delta_1)H^{**},\\
\gamma I^{**} + u_4 H^{**} &= (\mu + \omega)R^{**}.
\end{aligned} \tag{3.13}$$

So, taking the derivative of $\mathcal{V}$ with respect to t gives

$$\frac{d\mathcal{V}}{dt} = (S - S^{**})S' + (E - E^{**})E' + (I - I^{**})I' + (H - H^{**})H' + (R - R^{**})R'. \tag{3.14}$$

Substituting (2.1)*) into* (3.14) *as appropriate, we get*

$$\begin{aligned}
\frac{d\mathcal{V}}{dt} = \;& (S - S^{**})(\Lambda + \omega R - (1 - u_1)(\beta_1 E + \beta_2 H + \beta_3 I)S - \mu S)\\
&+ (E - E^{**})((1 - u_1)(\beta_1 E + \beta_2 H + \beta_3 I)S - u_2 E - \rho E - \mu E)\\
&+ (I - I^{**})(\rho E - (u_3 + \gamma + (\mu + \delta_2)I)\\
&+ (H - H^{**})(u_2 E + u_3 I - (u_4 + \mu + \delta_1)H)\\
&+ (R - R^{**})(\gamma I + u_4 H - \omega R - \mu R).
\end{aligned} \tag{3.15}$$

In addition, using the endemic equilibrium relations in (3.13) *as appro-*

priate in (3.15) *yields*

$$\begin{aligned}\frac{d\mathcal{V}}{dt} \leq\ & (S-S^{**})\big((1-u_1)(\beta_1E^{**}+\beta_2H^{**}+\beta_3I^{**})S^{**}+\mu S^{**}\\ & -(1-u_1)(\beta_1E+\beta_2H+\beta_3I)S-\mu S\big)\\ & +(E-E^{**})((u_2+\rho+\mu)E^{**}-(u_2+\rho+\mu)E)\\ & +(I-I^{**})((u_3+\gamma+\mu+\delta_2)I^{**}-(u_3+\gamma+\mu+\delta_2)I)\\ & +(H-H^{**})((u_4+\mu+\delta_1)H^{**}-(u_4+\mu+\delta_1)H)\\ & +(R-R^{**})((\omega+\mu)R^{**}-(\omega+\mu)R).\end{aligned} \tag{3.16}$$

On simplifying (3.16)*, we obtain*

$$\begin{aligned}\frac{d\mathcal{V}}{dt} \leq\ & -\big((1-u_1)(\beta_1(E^{**}-E)+\beta_2(H^{**}-H)+\beta_3(I^{**}-I))+\mu\big)(S-S^{**})^2\\ & -(u_2+\rho+\mu)(E-E^{**})^2-(u_3+\gamma+\mu+\delta_2)(I-I^{**})^2\\ & -(u_4+\mu+\delta_1)(H-H^{**})^2-(\omega+\mu)(R-R^{**})^2,\\ \leq\ & 0, \qquad if\ \mathcal{R}_0>1,\ while\ \varepsilon_2\ exists\ and\\ & \qquad E^{**}\geq E,\ I^{**}\geq I,\ H^{**}\geq H,\ R^{**}\geq R.\end{aligned} \tag{3.17}$$

We can infer from the preceding equations (3.16) *that* $\mathcal{V}'=0$ *only at* ε_2*. Hence, every solution to the model system of equations* (2.1) *with initial conditions in* Ω *tends to* ε_2 *as* $t\to\infty$ *if* $\mathcal{R}_0>1$ *. Therefore, the endemic equilibrium* ε_2 *is globally asymptotically stable if* $\mathcal{R}_0>1$ *going by the LaSalle's invariance principle [9].*

4 Numerical Results and Discussion

4.1 Estimation of Parameters

The average new recruitment per unit time (Λ) into the susceptible population was estimated using the annual increase in Nigeria's population from year 2000-2015. Nigeria's average annual population increase is estimated to be 3.922 million per year [15]. Thus, the daily new recruitment will be $\Lambda=\frac{3.922}{365}=0.0107$.

In order to estimate the daily death rate of Nigerians, we used the average life expectancy of Nigerians which is estimated as $\frac{1}{2}(53+56)=54.5$ years and the concept that an individual losses the reciprocal of its life expectancy every day. This implies that $\mu=\frac{1}{365\times54.5}=0.00005$ [17].

Using the half-life concept, we estimate the disease progression rate (ρ) into the symptomatic infected compartment based on the fact that about a fifth of asymptomatic infected individuals become symptomatic infected

while it takes a maximum of 14 days for this transition to take place. So, $\rho = -\frac{1}{14}\ln(0.2) = 0.155$ [16].

We estimated the natural recovery rate (γ) based on the fact that about 80% of infected individuals recover without treatment while an average of about a quarter infected individuals recover on daily basis [16, 12]. Thus, $\gamma = 0.8 \times 0.25 = 0.2$.

The disease-induced death rate (δ_1) is estimated from the Nigeria COVID-19 epidemiological data of 79 consecutive days [16]. So, we estimate it as $\delta_1 = \frac{1}{79} \times \ln\frac{506}{2} = 0.07$. In addition, we assumed that those COVID-19 infected individuals who were not hospitalized are twice likely to die due to the infection. Hence, $\delta_2 = 2 \times 0.07 = 0.14$.

Similarly, the disease transmission rate due to the exposed individuals (β_1) is estimated using the Nigeria COVID-19 prevalence epidemiological data of 79 consecutive days [16]. So, we estimated $6\beta_1 = \frac{1}{79} \times \ln\frac{19808}{190} = 0.0588$. Thus, $\beta_1 = 0.0098$. Also, we assume that the hospitalized infected individuals are twice likely to transmit the disease when compared to asymptomatic infected individuals while the undetected symptomatically infected individuals are three times likely to transmit the disease when compared to asymptomatic infected individuals. Hence, we estimate $\beta_2 = 2 \times \beta_1 = 0.0196$ and $\beta_3 = 3 \times \beta_1 = 0.0294$.

The disease waning rate ω is taken conservatively to be 0.005, since the outbreak is unprecedented in human history. It is worth mentioning that this term is incorporated based on recent reports of cases of re-infection by the disease after recovery in some countries. We assumed that it will take about six months before an earlier infected person could be re-infected.

4.2 Initial Condition of the Model

The proposed model was solved numerically using the Runge-Kunta fourth order scheme executed with MATLAB codes. We adopted the Nigerian coronavirus surveillance data for the 17th May, 2020. We assumed the total number of people tested for the virus as at the date as initial cohort for the disease spread through which the entire country might eventually become susceptible. So, we take the initial conditions for each of the compartments as $S(0) = 28193, E(0) = 1394, I(0) = 4183, H(0) = 4183, R(0) = 1594$ with model parameter values as estimated in the preceding section while we simulate different scenarios of the disease outbreak.

4.3 Results and Discussion

The numerical solution of the model (2.1) is obtained by using MATLAB with initial conditions and parameter values as stated earlier.

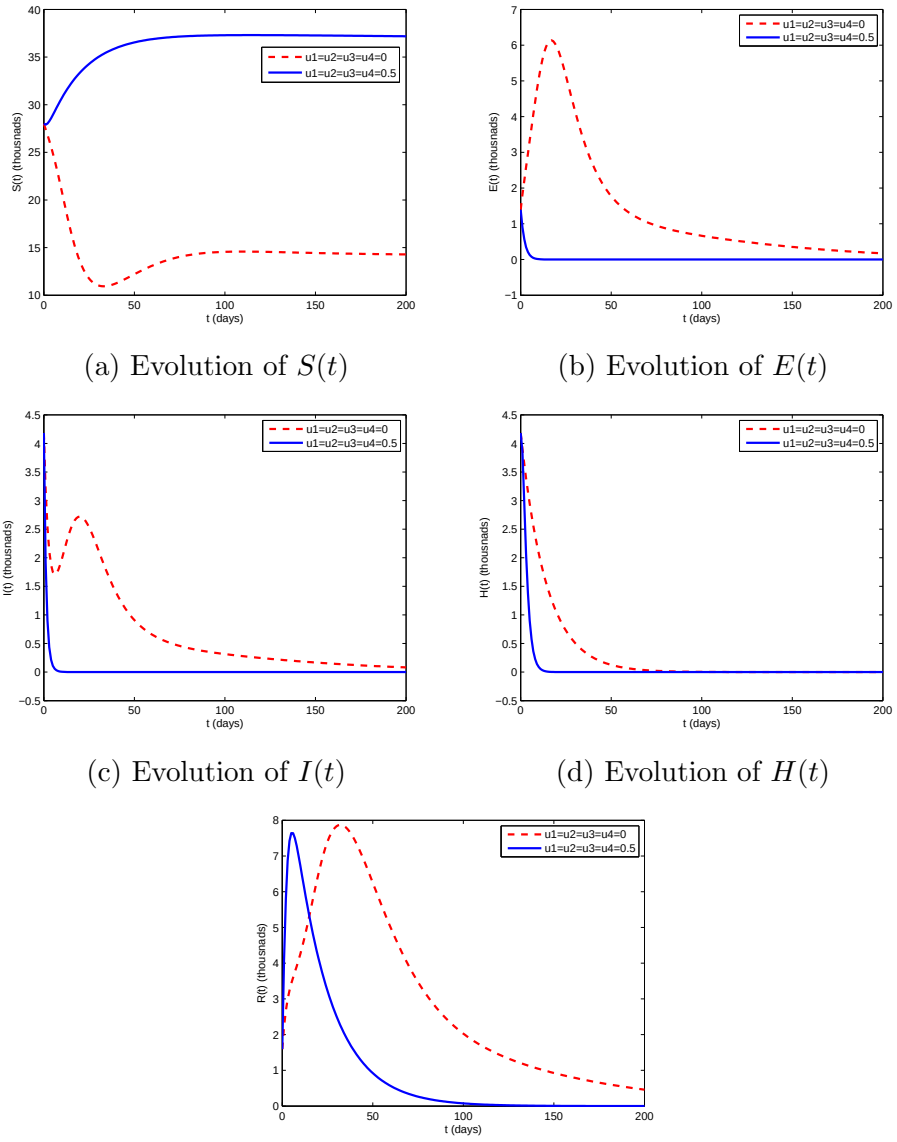

(a) Evolution of $S(t)$

(b) Evolution of $E(t)$

(c) Evolution of $I(t)$

(d) Evolution of $H(t)$

(e) Evolution of (t)

Figure 4.1: Population of each Model Compartment in Time with and without Control

Figure 4.1(a) shows that the introduction of the control measures, u_1, u_2, u_3

and u_4, leads to an increase in the number of individuals that are susceptible to the disease. This is expected because the implementation of these effective control measures reduces the number of susceptibles getting infected with the disease while equally increasing the number of individuals recovering from the disease. Thus, resulting in a significant increase in the number of individuals in the susceptible class as against the case when there is no control measure in place. As for this latter scenario, more of the susceptibles get infected while less of those who get infected recover due to higher mortality in such instances. So, less recovered individuals eventually become susceptible again after loosing their temporary immunity. Hence, the susceptible population in this latter case will be less when compared to a scenario with control measures in place.

In Figure 4.1(b), the uncontrolled scenario shows a steady increase in the number of humans that are exposed to COVID-19. However, the curve starts to fall after attaining a peak, possibly due to natural progression of individuals in this class into the symptomatic stage of the infection. Thus, a steady decrease is observed as the number of individuals in the class dwindle. On the other hand, the controlled scenario shows that the exposed class population experience a very sharp fall (without any rise) with time as it rapidly approaches zero within a very short period of time. This shows that this fall could not have been due to disease progression alone, but also as a result of the complemented impacts of the implemented control measures.

The uncontrolled scenario in Figure 4.1(c) shows an initial decrease and then a sudden rise in the population of symptomatic infected individuals with COVID-19 disease; thereafter there is a steady decrease in the class population over time. The initial decrease could be due to high mortality among the earlier infected individuals, while the sudden rise is possibly because the disease has spread rapidly before people get to know how best to protect themselves against it. On the contrary, the symptomatic infected population class continues to fall over time under the control scenario which could be due to impacts of the series of implemented control and preventive measures like ban on public gatherings, ban on interstate travels, minimization of work period, temporary closure of educational institutions, adherence to personal hygiene (hand washing and sanitizing), complying with social distancing, etc. Obviously, with all these measures, the number of new cases of the disease would reduce continuously over time while the number of symptomatic infected individuals would continue to fall too.

Figure 4.1(d) shows a steady decrease in the number of humans that are hospitalized due to COVID-19 infection in various designated isolation centres. As depicted in the plots, the scenario with control shows the hospitalized class population rapidly approaching zero within a relatively short

period of time while in the uncontrolled scenarios, it approaches zero at a slower rate, taking much longer time.

Figure 4.1(e) shows that the recovered class population peak attained under the uncontrolled scenario is higher than that of the controlled scenario while the rate at which the population falls afterward is much rapid in the latter than in the former. This could be due to the fact that lesser people get infected in the presence of disease control measures. So, only the few infected would need to recover while their recovery will be hastened since they would be under the care of medical experts.

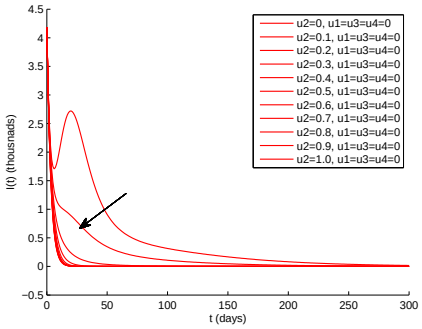

(a) Effects of Varying Control Measure u_2 on the Infected Population

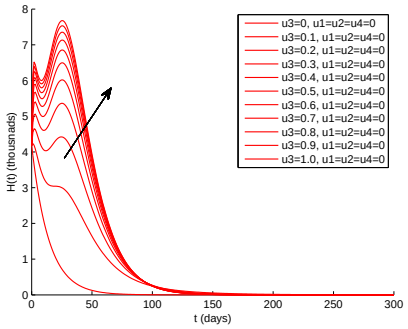

(b) Effects of Varying Control Measure u_3 on the Hospitalized Population

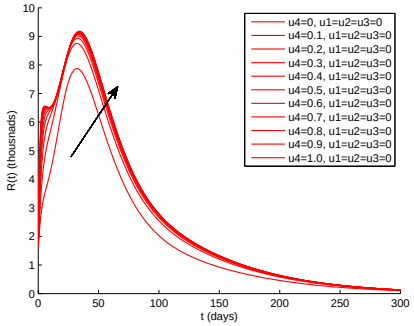

(c) Effects of Varying Control Measure u_4 on the Recovered Population

Figure 4.2: Effects of Varying Control Measures u_2, u_3 and u_4 on the Infected, Hospitalized and Recovered Population

Figure 4.2(a) shows that an increase in the success rate of contact tracing and testing of individuals in the exposed class (u_2) from $0 - 1$ leads to a decrease in the number of individuals that are symptomatic infected with

the disease. Moreover, the implication of this result is that if strategies can be put in place to effectively trace contacts of asymptomatic infected individuals for timely detection and isolation of the infected ones, there would be a remarkable reduction in the new cases of the disease. This is particularly important because there are apprehensions that this class of individuals is possibly the group fueling the spread of the disease. Hence, control strategies that address effective contact tracing and timely detection of asymptomatically infected individuals would help to flatten the disease curve within a short period of time and bring it under control.

Figure 4.2(b) shows that an increase in the successful detection rate of symptomatically infected individuals (u_3) from $0-1$ leads to an increase in the number of humans that are hospitalized due to COVID-19. This increase is rapid at the initial stage $u_3 = 0-0.5$. Thereafter, a steady increase is observed from $u_3 = 0.5-1$. The number of hospitalized individuals eventually approaches zero after about 200 days. In this case, majority of the hospitalized infected patients would have recovered while a few may eventually die in the process, thus justifying the population tending to zero afterwards.

Figure 4.2(c) shows that an increase in the success rate of medical care for hospitalized individuals (u_4) from $0-1$ leads to an increase in the number of people that recover from COVID-19. This increase is rapid at the initial stage $u_4 = 0-0.1$. This shows the advantage of being placed in isolation under the watch of medical experts. Thereafter, a steady increase is observed from $u_4 = 0.1-1$. The recovered population class eventually starts to fall approaching zero after about 200 days which could be attributed to the waning of temporary immunity enjoyed by individuals in the recovery class after about six months.

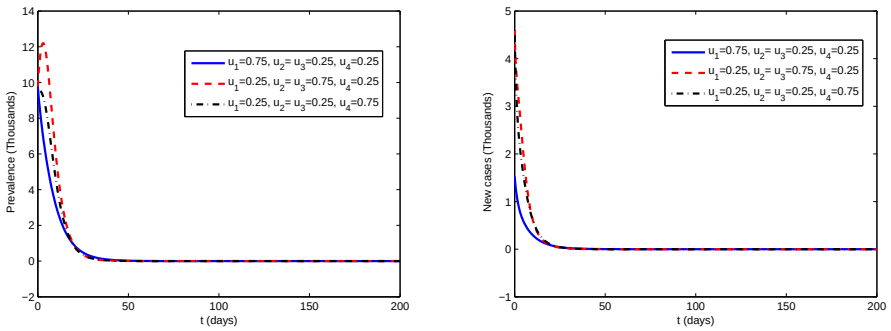

(a) Plot of Prevalence in Time (b) Plot of New Cases in Time

Figure 4.3: Effectiveness of different combinations of control measures on disease prevalence and new cases

Figure 4.3(a) shows the effects of varying combinations of the effectiveness of the different control measures ($u_1 - u_4$). The results indicate that the preventive control measure, u_1, is the most effective control measure (among the existing ones) in curtailing the spread of the disease. Hence, decision makers and government agencies should give priority to COVID-19 disease control and preventive protocols implementation in their strive to contain the pandemic. Moreover, highly effective implementation of the preventive protocols, when combined with minimal level of effectiveness of other measures, would help drive the disease prevalence towards extinction faster as compared to when any other control measure is given preference in the combination.

Figure 4.3(b) indicates that highly effective preventive control measures, when combined with some other measures with low level effectiveness, would be most effective in rapidly reducing the new cases of the disease. Thus, emphasis should be on ensuring that people comply with safety and preventive protocols, particularly in public places while the other control measures, hitherto implemented, should equally be sustained.

5 Concluding Remarks

In this paper, a five-dimensional deterministic model describing the impacts of precautionary measures (such as wearing face mask, observing social distance, and practising good hygiene), contact tracing and testing for exposed individuals, detection rate for symptomatic individuals, and hospitalization on the community spread of COVID-19 in Nigeria is presented. The effects of the four control measures are evaluated through numerical simulations. The simulated results suggest that the disease will diminish more rapidly in the population if about 50% of the population adhere to personal protection, contact tracing and testing is conducted on about 50% of exposed individuals daily with about 50% of symptomatic individuals successfully detected for isolation/hospitalization, and prompt management control is administered on about 50% of hospitalized individuals. It is therefore recommended that the combination of the four control interventions should be strictly adhered to.

Further work should include other control variables, especially vaccination since different vaccines with high level of efficacy have been made available and integrated to COVID-19 control strategy worldwide. However, joint implementation of several interventions is often costly, so it is necessary to derive the optimal levels of these interventions required to minimize the spread of COVID-19 at minimum cost using optimal control theory.

References

[1] Adegboye OA, Adekunle AI, Gayawan E. Early transmission dynamics of novel coronavirus (COVID-19) in Nigeria. International Journal of Environmental Research and Public Health. 2020;17(3054): 1–10. http://dx.doi:10.3390/ijerph17093054.

[2] Alanagreh L, Alzoughool F, Atoum M. The human coronavirus disease COVID-19: its origin, characteristics, and insights into potential drugs and its mechanisms. Pathogens. 2020;9(331): 1–11. http://dx.doi:10.3390/pathogens9050331.

[3] Al-Hussein AA, Tahir FR. Epidemiological characteristics of COVID-19 ongoing epidemic in Iraq. World Health Organization E-pub. 2020: 1–9. http://dx.doi.org/10.2471/BLT.20.257907

[4] Bulchandani VB, Shivam S, Moudgalya S, Sondhi SL. Digital herd immunity and COVID-19. MedRxiv. 2020:1–8. https://doi.org/10.1101/2020.04.15.20066720.

[5] Cakir Z, Savas HB. A mathematical modelling approach in the spread of the novel 2019 coronavirus SARS-CoV-2 (COVID-19) pandemic. Electronic Journal of General Medicine. 2020;17(4):1–3. https://doi.org/10.29333/ejgm/7861.

[6] Driessche P, Watmough J. Reproduction numbers and sub-threshold endemic equilibria for compartmental models of disease transmission, Mathematical Biosciences. 2002;180:29–48.

[7] Ivorra B, Ferrandezb MR, Vela-Perezc M, Ramosd AM. Mathematical modeling of the spread of the coronavirus disease 2019 (COVID-19) taking into account the undetected infections. The case of China. Interdisciplinary Mathematics Institute Complutense University of Madrid. 2020:1–29. https://doi.org/10.1016/j.cnsns.2020.105303.

[8] Kucharski AJ, Russell TW, Diamond C, Liu Y, Edmunds J, Funk S, Eggo RM. Early dynamics of transmission and control of COVID-19: a mathematical modelling study. Articles. 2020;20:553–558.

[9] LaSalle J, Lefschetz S. The stability of dynamical systems, *SIAM, Philadelphia*. 1976.

[10] Li Y, Wang B, Peng R, Zhou C, Zhan Y, Liu Z, Jiang X, Zhao B. Mathematical modeling and epidemic prediction of COVID-19 and its

significance to epidemic prevention and control measures. Research Article. 2020;5(1): 1–9.

[11] Liu Y, Gayle AA, Wilder-Smith A, Rocklov J. The reproductive number of COVID-19 is higher compared to SARS coronavirus. Journal of Travel Medicine. 2020;1–4.
https://doi: 10.1093/jtm/taaa021

[12] Nigeria Centre for Disease Control (2022). COVID-19 Outbreak in Nigeria situation report; NCDC: Abuja, Nigeria, 2022. (Accessed on 25th February, 2022).

[13] Okhuese VA. Mathematical predictions for COVID-19 as a global pandemic. *MedRxiv*, 2020;1–16.
https://doi.org/10.1101/2020.03.19.20038794.

[14] Rothana HA, Byrareddy SN. The epidemiology and pathogenesis of coronavirus disease (COVID-19) outbreak. Journal of Autoimmunity. 2020;1–4.
https://doi.org/10.1016/j.jaut.2020.102433.

[15] United Nation (2017). World population prospects. https://esa.un.org/unpd/wpp/DataQuery/

[16] World Health Organization. Coronavirus disease (COVID-2019) situation reports, 2022. Available online: https://www.who.int/emergencies/diseases/novel-coronavirus-2019/situation-reports (Accessed on 25th February, 2022, 2020).

[17] Yusuf TT. Mathematical modelling and simulation of Meningoccal Meningitis transmission dynamics. FUTA Journal of Research in Sciences. 2018;14(1):94–104.

[18] Zhao S, Linc Q, Rand J, Musae SS, Yangf G, Wangh W, Loue Y, Gaoi D, Yangj L, Hee D, Wang MH. Preliminary estimation of the basic reproduction number of novel coronavirus (2019-nCoV) in China, from 2019 to 2020: a data-driven analysis in the early phase of the outbreak. International Journal of Infectious Diseases. 2020;92 (2020):214–217.
https://doi.org/10.1016/j.ijid.2020.01.050.

[19] Zafar ZUA, Hussain MT, Inc M, Baleanu D, Almohsen B, Oke AS, Javeed S. Fractional-order dynamics of human Papillomavirus. Results in Physics. 2022;34(3):105281.

[20] Oke AS, Bada OI, Rasaq G, Adodo V. Mathematical analysis of the dynamics of COVID-19 in Africa under the influence of asymptomatic cases and re-infection. Mathematical Methods in the Applied Sciences. 2022;45(1):137–149.

[21] Oke AS, Bada OI, Rasaq G, Adodo V, Juma BA. COVID-19 dynamics in Africa under the influence of asymptomatic cases and re-infection. International Journal of Mathematical Modelling and Computations. 2021. DOI: 10.22541/au.159799145.54759313

[22] Bada OI, Oke AS, Mutuku WN, Aye PO. Analysis of the dynamics of SI-SI-SEIR avian influenza A(H7N9) epidemic model with re-infection. Earthline Journal of Mathematical Sciences. 2021;5(1):43–73.

[23] Oke AS, Bada OI. Analysis of the dynamics of avian influenza A(H7N9) epidemic model with re-infection. Open Journal of Mathematical Sciences. 2019;3(1):417–432.

[24] Adamu G, Ibrahim MO, Ejieji CN, Yusuf HB. Mathematical modelling and vaccination acceptability analysis of COVID-19 in Nigeria. Mathematics and Computational Sciences. 2021;2(4):24–40.

[25] Ugwu CS. Mathematical model on gonorrhoea transmission, M.Sc. Dissertation, University of Nigeria, Nsukka. 2015.

[26] Abidemi A, Aziz NAB. Analysis of deterministic models for dengue disease transmission dynamics with vaccination perspective in Johor, Malaysia. International Journal of Applied and Computational Mathematics. 2022;8(1):1–51.

[27] Abidemi A, Ahmad R, Aziz NAB. Assessing the roles of human movement and vector vertical transmission on dengue fever spread and control in connected patches: from modelling to simulation. The European Physical Journal Plus. 2021;136(11):1–32.

[28] Abidemi A, Zainuddin ZM, Aziz NAB. Impact of control interventions on COVID-19 population dynamics in Malaysia: a mathematical study. The European Physical Journal Plus. 2021;136(2):1–35.

[29] Asamoah JKK, Okyere E, Abidemi A, Moore SE, Sun GQ, Jin Z, Acheampong E, Gordon JF. Optimal control and comprehensive cost-effectiveness analysis for COVID-19. Results in Physics. 2022:105177.

[30] Dansu EJ, Ogunjo ST. Dynamics of inter-community spread of COVID-19, in: Agarwal P, Nieto PP, Ruzhansky M, Torres DFM (Eds.), Analysis of Infectious Disease Problems (Covid-19) and Their Global Impact, Springer, 2021, pp. 409–426.

[31] Kanyi E, Afolabi AS, Onyango NO. Mathematical modeling and analysis of transmission dynamics and control of schistosomiasis. Journal of Applied Mathematics. 20221;2021:1–20.

[32] Kanyi E, Afolabi As, Onyango NO. Optimal control analysis of schistosomiasis dynamics. Journal of Mathematical and Computational Science. 2021;11(4):4599–4630.

[33] Idisi OI, Yusuf TT. A mathematical model for Lassa fever transmission dynamics with impacts of control measures: analysis and simulation. European Journal of Mathematics and Statistics. 2021;2(2):19-28.

[34] Yusuf TT. On global stability of disease-free equilibrium in epidemiological models. European Journal of Mathematics and Statistics. 2021;2(3):37-42.

[35] Yusuf TT, Idisi OI. Modelling the transmission dynamics of HIV and HBV coepidemics: analysis and simulation. Mathematical Theory and Modeling. 2020;10(2):48-77.